JOURNAL OF BACTERIOLOGY, Oct. 2005, p. 7027–7037 Vol. 187, No. 20
0021-9193/05/$08.00+0 doi:10.1128/JB.187.20.7027–7037.2005

Analysis of Global Gene Expression and Double-Strand-Break Formation in DNA Adenine Methyltransferase- and Mismatch Repair-Deficient *Escherichia coli*†

Jennifer L. Robbins-Manke,[1] Zoran Z. Zdraveski,[2] Martin Marinus,[3] and John M. Essigmann[1,2]*

Biological Engineering Division, Massachusetts Institute of Technology, Cambridge, Massachusetts 02139[1]; Department of Chemistry, Massachusetts Institute of Technology, Cambridge, Massachusetts 02139[2]; and Department of Biochemistry and Molecular Pharmacology, University of Massachusetts Medical School, Worcester, Massachusetts 01605[3]

Received 4 June 2005/Accepted 1 August 2005

DNA adenine methylation by DNA adenine methyltransferase (Dam) in *Escherichia coli* plays an important role in processes such as DNA replication initiation, gene expression regulation, and mismatch repair. In addition, *E. coli* strains deficient in Dam are hypersensitive to DNA-damaging agents. We used genome microarrays to compare the transcriptional profiles of *E. coli* strains deficient in Dam and mismatch repair (*dam*, *dam mutS*, and *mutS* mutants). Our results show that >200 genes are expressed at a higher level in the *dam* strain, while an additional mutation in *mutS* suppresses the induction of many of the same genes. We also show by microarray and semiquantitative real-time reverse transcription-PCR that both *dam* and *dam mutS* strains show derepression of LexA-regulated SOS genes as well as the up-regulation of other non-SOS genes involved in DNA repair. To correlate the level of SOS induction and the up-regulation of genes involved in recombinational repair with the level of DNA damage, we used neutral single-cell electrophoresis to determine the number of double-strand breaks per cell in each of the strains. We find that *dam* mutant *E. coli* strains have a significantly higher level of double-strand breaks than the other strains. We also observe a broad range in the number of double-strand breaks in *dam* mutant cells, with a minority of cells showing as many as 10 or more double-strand breaks. We propose that the up-regulation of recombinational repair in *dam* mutants allows for the efficient repair of double-strand breaks whose formation is dependent on functional mismatch repair.

The DNA adenine methyltransferase (Dam) protein methylates the N6 position of the adenine residue at d(GATC) sites of the *Escherichia coli* genome. Dam methylation is a postreplicative process (28), and consequently the newly synthesized daughter strand is unmethylated for a short time after passage of the replication fork. This transient hemimethylated state following DNA replication plays a crucial role in processes such as the regulation of gene expression (11, 26, 45), DNA mismatch repair (3, 45, 55), and the timing of chromosome replication initiation (2, 24, 42, 52). By altering the recognition sequences of transcriptional regulators and RNA polymerases, Dam methylation may affect the ability of proteins to bind the upstream regions of genes and in such a way may serve to regulate gene expression. Because d(GATC) sites are not randomly distributed in the *E. coli* genome (19, 44), Dam deficiency may therefore have a direct effect on gene expression patterns.

In methyl-directed mismatch repair, hemimethylated d(GATC) sites serve as the strand discrimination signal so that mismatch repair can differentiate between parent (methylated) and daughter (unmethylated) strands (38). The mismatch repair system relies on three unique proteins: MutS, MutL, and MutH. If there is a misincorporation error following the replication fork, MutS recognizes the mismatch, and a protein-DNA complex is formed with MutS, MutL, and the latent endonuclease MutH. Activated MutH then makes an incision on the unmethylated, or newly synthesized, strand at a d(GATC) site located either 5′ or 3′ to the mismatch (1, 10, 18). Methylation status therefore allows mismatch repair to act on the new strand while preserving the sequence of the template strand, and in this way mismatch repair helps protect the genome against mutations arising from misincorporated deoxynucleotides. In the case where Dam is absent and the genome is unmethylated at d(GATC) sites, MutH cannot distinguish between the new and template strands; in vitro experiments show that in this situation MutH aimlessly makes an incision on either strand, although the endonuclease shows reduced activity on unmethylated compared to hemimethylated substrates (1, 63). Furthermore, Au et al. (1) have shown in a reconstituted in vitro system that in the absence of d(GATC) methylation MutH can make incisions on both DNA strands and form a double-strand break (DSB).

E. coli strains deficient in Dam exhibit pleiotropic changes that have helped uncover many functions of adenine methylation. Dam-deficient strains display a mutator phenotype (30), which most likely results from mismatch-repair activity on the template rather than daughter strands following replication errors. Interestingly, a mutator phenotype is also conferred by the overexpression of Dam (20, 64), which may result in fully methylated DNA following the replication fork that is resistant

* Corresponding author. Mailing address: Biological Engineering Division, Massachusetts Institute of Technology, 77 Massachusetts Ave., 56-670, Cambridge, MA 02139. Phone: (617) 253-6227. Fax: (617) 253-5445. E-mail: jessig@mit.edu.

† Supplemental material for this article may be found at http://jb.asm.org/.

TABLE 1. Genotypes of *E. coli* K-12 strains used in this study

Strain	Genotype	Source
AB1157	F$^-$ *thr-1 araC14 leuB6*(Am) Δ(*gpt-proA*)*62 lacY1 tsx-33 supE44*(AS) *galK2*(Oc) *hisG4*(Oc) *rfbD1 mgl-51 rpoS396*(Am) *rpsL31*(Str^r) *kdgK51 xylA5 mtl-1 argE3*(Oc) *thi-1*	DeWitt and Adelberg (13)
GM3819	*dam-16*::Kan *thr-1 leuB6 thi-1 argE3 hisG4 proA2 lacY1 galK2 mtl-1 xyl-5 ara-14 rpsL31 tsx-33 supE44 rfbD1 kdgK51*	Parker and Marinus (46)
GM5555	As AB1157 but *mutS215*::Tn*10*	Laboratory stock
GM5556	As GM3819 *dam-16*::Kan but *mutS215*::Tn*10*	Laboratory stock

to MutH incision. Other studies have shown that the SOS response is constitutively induced (subinduced) in the absence of Dam (43, 49, 53). The induction of SOS response genes in *dam* mutant strains may be due to the presence of single-stranded DNA resulting from errant MutH incisions. However, *dam mutS*/*L*/*H* strains in which mismatch repair is inactivated also show SOS subinduction (48). Dam-deficient *E. coli* strains are also hyperrecombinogenic (29, 31), and double mutants deficient in both Dam and recombinational repair (*dam recA*, *-B*, and *-C* and *dam ruvA*, *-B*, and *-C*) are inviable (27, 30, 48, 62). Wang and Smith (62) have shown that the requirement for recombination in *dam E. coli* is correlated to the mismatch repair-dependent production of DSBs, and accordingly mutations in mismatch repair (*mutL* or *mutS*) allow the recovery of *dam rec* mutants.

Wang and Smith (62) determined the relative levels of DSBs in *dam*, *recB*(Ts) (a temperature-sensitive mutant), *dam recB*(Ts), and *dam recB*(Ts) *mutS*/*L* cells; they could only detect DSBs in the *dam recB*(Ts) strain and not in the *dam* mutation-only cells. However we expect *dam*-only mutant cells to exhibit a higher level of DSBs than the wild type because *dam* mutants deficient in DSB repair are inviable (27, 30, 49). Furthermore, *dam* mutants are hypersensitive to exogenous DNA-damaging agents and this hypersensitivity is abrogated by an additional mutation in mismatch repair (16); this hypersensitivity may be due to basal differences in *dam* mutants that, like DSB formation, are dependent on mismatch repair. In order to help elucidate the global changes resulting from Dam deficiency and the role of mismatch repair in producing these changes, we determined the global gene expression profiles of wild-type, *dam*, *dam mutS*, and *mutS E. coli* strains by microarray analysis of ~4,200 open reading frames. We also measured the number of DSBs in each of the strains and correlated the level of basal DNA damage with the induction of genes involved in recombination and DSB repair. Our findings show that many genes involved in carbohydrate metabolism and transport, energy production and conversion, cell motility, and translation are up-regulated in *dam* mutant *E. coli*, whereas an additional mutation in *mutS* suppresses gene induction. We also see up-regulation of several SOS response genes in both *dam* and *dam mutS* mutants. However, only the *dam* mutant cells show a higher level of DNA DSBs compared to the wild type, and double-strand-break formation in *dam* mutant *E. coli* is dependent on functional mismatch repair.

MATERIALS AND METHODS

Bacterial strains. The strains used in this study are derivatives of AB1157, and the complete genotypes are listed in Table 1. We used the *dam-16*::Kan strain (GM3819), which carries a deletion of a large part of the *dam* gene. The auxotrophic phenotype of each mutant was confirmed by growth on the appropriate supplemented minimal medium.

Array analysis. (i) Total RNA isolation and purification. Overnight cultures were diluted 1,000-fold with fresh LB medium and cultured further. Log-phase cultures were diluted to a cell density of 2×10^8 cells/ml in M9 salts and incubated at 37°C for 2 h, after which they were resuspended in LB broth for 90 min. This treatment served as a mock treatment for cultures incubated with a chemical (cisplatin) in a parallel study (J. L. Robbins-Manke et al., unpublished results). Optical densities at 600 nm were measured, and total RNA was isolated from cells by extraction using the MasterPure RNA purification kit (Epicenter Technologies) followed by DNase digestion according to the manufacturer's protocol. The isolated total RNA was quantitated by absorption at 260 nm (typical yield from a 15-ml culture was 250 to 500 μg of total RNA), and the purity was determined by the ratio of absorption values at 260/280 nm. RNA quality was determined by formaldehyde agarose gel electrophoresis (1.2% agarose in FA buffer, pH 7.0, which contains 20 mM 3-[*N*-morpholino]propanesulfonic acid, 5 mM sodium acetate, and 1 mM EDTA) or by analysis on an Agilent 2100 bioanalyzer. All samples visualized by gel electrophoresis or by the bioanalyzer electropherogram showed clear distinct bands correlating to 16S and 23S rRNA, indicating that no detectable RNA degradation occurred and that RNA integrity was maintained throughout the RNA isolation procedure (data not shown).

(ii) mRNA enrichment, fragmentation, and labeling for arrays. mRNA was enriched from total RNA as described in the *Affymetrix GeneChip Expression Analysis Technical Manual for GeneChip E. coli Sense Genome Arrays* (Affymetrix, Santa Clara, CA). In brief, reverse transcriptase and primers specific to 16S and 23S rRNA were used to synthesize complementary cDNAs. Then rRNA was removed by treatment with RNase H (Epicenter Technologies), which specifically digests RNA within an RNA-DNA hybrid. The cDNA molecules were removed by DNase I (Amersham Biosciences) digestion, and the enriched mRNA was purified on QIAGEN RNeasy columns according to the manufacturer's protocol. Enriched mRNA was then fragmented by heat and ion-mediated hydrolysis. The 5′-end RNA termini were then modified by T4 polynucleotide kinase (New England Biolabs) and γ-S-ATP (Boehringer Mannheim). Next a biotin group (PEO-iodeacetyl-biotin; Pierce Chemical) was conjugated to 5′ ends of the RNA. The conjugated product was purified using an RNA/DNA Mini column kit (QIAGEN), and the efficiency of the labeling procedure was determined by a gel-shift assay on a 4 to 20% Tris-borate-EDTA gel (Invitrogen; data not shown). Target hybridization and probe array washing, staining, and scanning were performed as described in the *Affymetrix Manual*.

(iii) Data analysis. Experiments for array analysis were performed in biological replicates with three independent experiments for each strain. Signal intensities of each array were normalized by the Robust Multi-array Average (RMA) version 0.1 release (5, 21), and normalized signal intensities for each gene were averaged across the three biological replicates for each strain. Changes in gene expression are given as signal log ratios (base 2), and analysis of variance (ANOVA) was used to compare gene expression values in each mutant strain, using wild-type *E. coli* as the baseline for comparison. All microarray data analysis (i.e., RMA normalization and ANOVA) was performed using the Array Analyzer module version 1.1 in S-Plus (Insightful) version 6.0. Transcripts were filtered based on a *P* value threshold of 0.05 as well as a fold change threshold of 2 (signal log ratio, $1 \leq x \leq -1$). Differentially regulated genes were annotated and categorized according to general function by the NCBI Clusters of Orthologous Groups (COG) database. We determined the number of d(GATC) sites in the promoter/regulatory regions of genes differentially expressed in our analysis by searching the upstream sequence regions (−400 bp from the transcriptional start site) of each gene. The sequences searched were provided on *coli*base (http://colibase.bham.ac.uk/), and the number of expected GATC sites occurring by chance in 400 bp was taken from Oshima et al. (44) and estimated to be one

GATC site every 256 bp (or between one and two sites in the searched regions). Raw microarray data and RMA-normalized data are available at the NCBI Gene Expression Omnibus (GEO) repository under accession no. GSE2928.

Semiquantitative real-time RT-PCR. Total RNA was isolated from cultures, and RNA quality was determined as described above. DNase digestion for total RNA was performed using amplification-grade DNase I (Invitrogen). Briefly, total RNA was incubated with 1 U DNase I per microgram RNA in 200 mM Tris-HCl, pH 8.4, 20 mM $MgCl_2$, 500 mM KCl for 15 min at room temperature. The reaction was terminated by the addition of EDTA (2 mM final concentration) and by heating for 10 min at 65°C. cDNA synthesis was performed using random hexamer primers (Invitrogen) and the Omniscript reverse transcriptase kit (QIAGEN) according to the manufacturer's protocol. In order to ensure that the amplification observed in the PCRs was due to cDNA template made from mRNA and not from contaminating genomic DNA, controls were carried out for each sample under the same conditions, except that reverse transcriptase was not added to the reactions. Semiquantitative real-time PCRs were performed with QuantiTect SYBR green (QIAGEN) according to the manufacturer's protocol on a DNA Engine Opticon thermal cycler (MJ Research). Primers specific to each target gene were designed using Primer3 software (http://www genome.wi.mit.edu/cgi-bin/primer/primer3.cgi/): *recA* left (5′-TACAGCTACAA AGGTGAGAAGATCG-3′) and *recA* right (5′-TTCGCTATCATCTACAGAG AAATCC-3′), *lexA* left (5′-GCATATTGAAGGTCATTATCAGGTC-3′) and *lexA* right (5′-ACCGTTACGTACATCCTGAGTTTT-3′), *recN* left (5′-GTAC AGCTGTTCCTCTGTCACAAC-3′) and *recN* right (5′-GTCATTTCCTGCAG TAGAGAGGTT-3′), *sulA* left (5′-CAACTTCTACTGTTGCCATTGTTAC-3′) and *sulA* right (5′-AGAGCTGGCTAATCTGCATTACTT-3′), *yebG* left (5′-C GAAGAGAAAATGTCGTTTACCAG-3′) and *yebG* right (5′-CTCAGCACA TCTTTTTGTTCTGC-3′), *dinI* left (5′-AGTATGCGTTTCCTGATAATGAA GG-3′) and *dinI* right (5′-TATTCGCTGACAAACCAGTCAT-3′), *uvrA* left (5′-ATAAAGTGGTGTTGTACGGTTCTG-3′) and *uvrA* right (5′-CACGGAC GATTACTGATAAACTTG-3′), *uvrB* left (5′-GTTTCCACTATTCCACGTTT TACC-3′) and *uvrB* right (5′-GTAGTTTTCAATCCCCGAACAGTA-3′), *cho* left (5′-GTGGTACGGCGTTTAACTTCTC-3′) and *cho* right (5′-GTTAACG CTTTTGCCGATATAGAG-3′), *ruvA* left (5′-CCTGTTTTTATGAACTCCCT GAAG-3′) and *ruvA* right (5′-CTCAACGGCATTAACGAACTG-3′), *ruvB* left (5′-GTTCGTTCACAGATGGAGATTTTC-3′) and *ruvB* right (5′-GATCTCA TCAATAAACAGCACGTC-3′), *hupA* left (5′-ATGCTGTACAACTGGTTGG TTTC-3′) and *hupA* right (5′-TTACTTAACTGCGTCTTTCAGTGC-3′), *hupB* left (5′-AGGGGCTGATATCTCTAAAGCTG-3′) and *hupB* right (5′-AAAAG TACCAAAACCTACCAGTGC-3′), *priA* left (5′-GTGTGATTTAGCAAGTG AAACACC-3′) and *priA* right (5′-TTTCCAGTACGCTGAGATAAACCT-3′), *priB* left (5′-GAAAGGTCAGTCCATCAGGAAT-3′) and *priB* right (5′-CCGA CCGTTATACTGTGAGTAATG-3′), and *gapA* left (5′-TATGACTGGTCCG TCTAAAGACAA-3′) and *gapA* right (5′-GGTTTTCTGAGTAGCGGTAGTA GC-3′). Optimal melting temperatures for each primer pair were determined by performing real-time analysis with a temperature gradient ranging over 10° (±5°C from the optimal calculated melting temperature for each primer pair), and negative controls with no template cDNA were performed to ensure that primers alone did not yield an amplification product. Relative gene expression values for the samples were measured by including a standard curve analysis for each gene assay; a separate batch of wild-type cDNA template was used to make a series dilution, and amplified product from this dilution series was used to make a standard curve by which to quantify the relative amount of product in each experimental sample. To account for variation in the efficiency of the reverse transcription (RT) reaction between samples, we performed RT-PCR for the constitutively expressed *gapA* (D-glyceraldehyde 3-phosphate dehydrogenase) gene and normalized the gene expression values detected in each sample to the value determined for *gapA*. Each experiment was carried out in triplicate, so each relative gene expression value reported for each strain represents the average of three independent biological replicates. Student's *t* test (two sample, two tailed) was used to determine if the expression values of a given gene were significantly different between strains.

Neutral single-cell gel electrophoresis. Cultures were grown as described above. Microgel electrophoresis was performed as described in detail by Singh et al. (56–58). Briefly, small aliquots (0.25 μl) of cells were mixed with 50 μl of 0.5% agarose (biotechnology grade 3:1; Amresco). Agarose containing cells was then immediately transferred to an MGE microscope slide (Erie Scientific, Portsmouth, NH) precoated with 50 μl agarose, and after cooling, another layer of agarose (200 μl) containing 5 μg/ml RNase A (Amresco), 0.25% sodium *N*-lauroyl sarcosine, and 0.5 mg/ml lysozyme (Amresco) was added with a coverglass. Slides were incubated at 4°C for 10 min, after which they were transferred to a humidified chamber at 37°C and incubated for 30 min. Coverglasses were then removed, and the slides were immersed in lysis buffer (2.5 M NaCl, 100 mM EDTA tetrasodium salt, 10 mM Tris, pH 10, 1% sodium *N*-lauroyl sarcosine, 0.1% Triton X-100) and incubated for 8 h. Slides were then immersed in buffer for protein digestion (2.5 M NaCl, 10 mM EDTA, 10 mM Tris, pH 7.4) containing 1 mg/ml proteinase K for 2 h at 37°C. After protein digestion, the slides were placed in a modified electrophoresis unit (TECA 2222; Ellard Instrumentation, Monroe, WA) with buffer (300 mM sodium acetate, 100 mM Tris, pH 9) and allowed to equilibrate for 20 min, after which electrophoresis was performed for 1 h at 12 V (0.4 V/cm) with buffer recirculation at 100 ml/min. Following electrophoresis, slides were incubated in solution containing 1:1 ethanol–20 mM Tris, pH 7.4, containing 1 mg/ml spermine for 30 min, and slides were then transferred to fresh solution for another 30 min. Slides were allowed to air dry until analysis. Dried slides were stained with 50 μl of 0.25 μM YOYO-1 iodide (Molecular Probes) in 2.5% dimethyl sulfoxide and 0.5% sucrose and immediately viewed on a Nikon Eclipse E600 fluorescence microscope equipped with a ×100/1.25 oil-immersion Fluor lens and a B-2A filter set (exciter, 490 nm; emitter, 515 nm). Three to six independent experiments were performed for each strain, and each experiment consisted of two slides per strain with at least 100 observations taken per slide, giving a total of at least 600 observations per strain. Pictures were analyzed with Komet analysis software version 4.0.2 (Kinetic Imaging Ltd.) and by visually counting individual strand breaks or tails for each cell. The frequency at which no DSBs occurred, one DSB occurred, and so on was determined for each strain. To determine if the frequencies at which DSBs occurred between the mutant and wild type were different, we performed the Mann-Whitney U test to compare the frequency of DSBs in each mutant strain to the frequency observed in the wild type.

RESULTS

Dam-deficient strains show a higher number of basal gene expression changes than the *mutS* strain. We measured the global gene expression patterns in four *E. coli* strains, using the Affymetrix microarray platform. We isolated mRNA from three independent biological replicate cultures for the wild-type, *dam*, *dam mutS*, and *mutS* strains, and the gene expression values from the replicates were averaged. Gene expression changes in mutant strains are given as signal log ratios (mutant/wild type, log base 2), and ANOVA was performed to compare gene expression levels in each of the mutant strains to the gene expression levels measured in wild-type *E. coli*. Figures 1A to C show the log *P* value versus signal log ratio for all transcripts: the bold lines mark the boundaries by which the data were filtered, the bold horizontal line represents the *P* value threshold, and the two bold vertical lines mark the signal log ratio threshold applied to the data. Genes whose expression shows at least a ±2-fold change compared to the wild type (signal log ratio, ±1) with a *P* value of ≤0.05 are represented in Fig. 1D and 1E (and see Tables S1 to S3 in the supplemental material). When we compare the basal gene expression differences between each of the mutant strains and the wild type, the results show that while the *mutS* strain does not display many differences from the wild type at the transcriptional level, both *dam* and *dam mutS* strains show differential expression of 206 and 114 genes, respectively. The majority of genes differentially expressed are expressed at higher levels (induced) in the mutant strains compared to the wild type (Fig. 1D). Among the most prominent groups of up-regulated genes are those encoding ribosomal subunit proteins and products involved in carbohydrate transport and metabolism (Fig. 1E). In particular, several genes encoding proteins in the sugar phosphotransferase system and maltose transport are up-regulated in the Dam-deficient strains. *dam* mutant *E. coli* strains also show up-regulation (≥2-fold induction, $P \leq 0.05$) of many genes involved in energy production and conversion (24 genes); cell motility (17 genes), including flagellar biosynthesis; amino acid

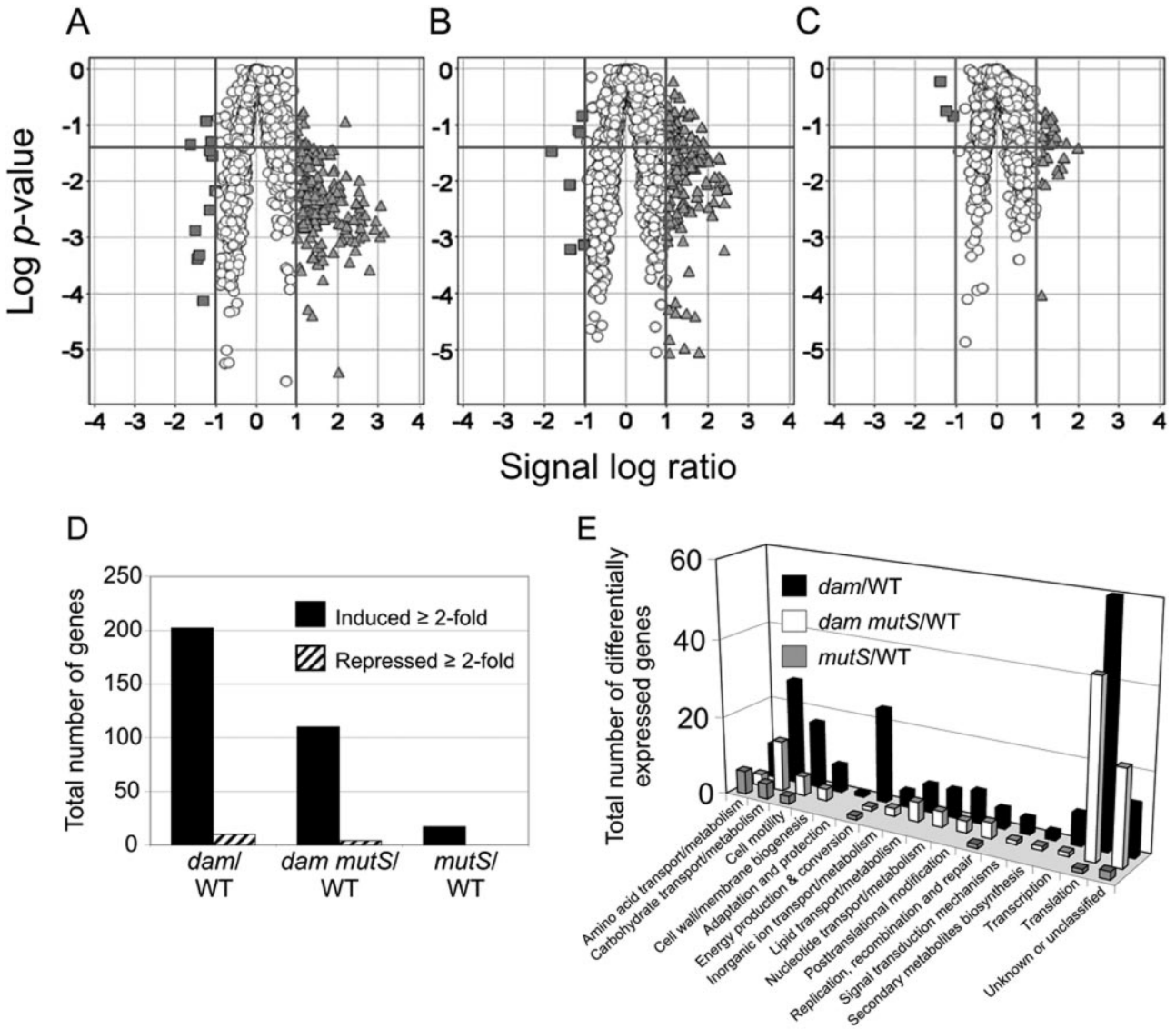

FIG. 1. Global transcriptional changes in *dam*, *dam mutS*, and *mutS E. coli* compared to the wild type (WT). ANOVA was performed using the wild-type expression level as a baseline, and log *P* values are plotted against signal log ratios for *dam* (A), *dam mutS* (B), and *mutS* (C) mutant cells. Circles represent genes that do not meet the twofold cutoff marked by the vertical bold lines, dark gray squares represent genes expressed at a twofold-lower level, and light gray triangles represent genes expressed at a twofold-higher level compared to the wild type. The horizontal bold line shows the *P* value threshold applied to filter the data ($P \leq 0.05$), and panels D and E show the filtered data. (D) Total number of genes induced/repressed twofold in each of the strains. Only genes for which the magnitude of induction or repression is at least twofold (signal log ratios of ≥ 1 and ≤ -1) and for which *P* is ≤ 0.05 are represented. (E) Genes in panel D are categorized according to general function as provided by the NCBI COG database.

transport and metabolism (9 genes); and transcription (8 genes), as well as genes of unknown function (12 genes). *dam mutS E. coli* strains also show up-regulation of genes involved in cell motility (5 genes) and genes of unclassified or unknown function (24 genes).

The higher level of global transcription in the Dam-deficient strains may be due to genes whose regulation is directly controlled by adenine methylation. While some transcriptional activators bind unmethylated DNA (7), the absence of Dam methylation may lead to the up-regulation of genes whose promoters/regulatory regions are normally methylated and therefore whose transcriptional activators are usually bound only following replication when the DNA is transiently unmethylated. Alternatively, genes whose repressors require adenine methylation for DNA binding affinity may also be up-regulated in the absence of Dam. Under such scenarios, Dam deficiency would directly affect the transcription of genes and would lead to increased gene expression. Although we were unable to find a correlation between gene expression level and the presence of d(GATC) sites in upstream sequence regions (−400 bp from the transcriptional start sites) in *dam* or *dam mutS* strains (see Tables S1 and S2 in the supplemental material), we do see expression changes of certain genes known to be regulated in a Dam methylation-dependent manner. For

example, *dnaA* expression is reduced in both *dam* and *dam mutS* strains (signal log ratio = −0.368, $P = 0.035$, and −0.412, $P = 0.025$, respectively), as shown previously in *dam* mutant strains (8, 25). Methylation of d(GATC) sites in the dnaAp2 promoter, two of which are in the −35 and −10 sequences, may affect the affinity of DNA binding proteins that regulate the expression of *dnaA* (8, 12). In addition, we find expression of the phase variation *flu* gene (*agn43*) to be slightly downregulated (signal log ratio = −0.383, $P = 0.016$) in *dam* mutant *E. coli*. While *agn43* transcription is controlled in a methylation-dependent manner, it is DNA methylation of three d(GATC) sites in the regulatory region that prevents binding of the repressor OxyR and that therefore leads to *agn43* expression and the ON phase (11, 61). Løbner-Olesen et al. (25) have shown that a 10-fold overproduction of Dam leads to a 20-fold induction of *flu* expression.

The effects of MutS on gene expression in a *dam* mutant background: differences between *dam* and *dam mutS* strains Both *dam* and *dam mutS* strains show a high level of gene induction compared to the wild type (Fig. 1A and B). The *dam mutS* strain, however, shows higher variability among some of these induced genes (Fig. 1B); specifically, 39 genes that show twofold-higher expression in the *dam mutS* mutant compared to the wild type are filtered out of the data set due to their high variability (i.e., they do not meet the *P* value threshold), and of these 39 genes 15 encode ribosomal proteins. The remaining genes are mostly involved in protein and carbohydrate metabolism. Data in Fig. 1D and 1E show the filtered data set that includes genes showing at least a ±twofold change with $P \leq 0.05$. Figure 1E shows that many of the expression changes in *dam* and *dam mutS* strains fall under common categories, with carbohydrate transport/metabolism and translation accounting for close to 50% of the transcriptional changes in these strains. Many of the genes induced in the *dam mutS* strain are also induced in the *dam* strain; that is, the genes induced in the *dam* strain include the majority of the genes induced in the *dam mutS* strain, and it is the case that the *dam* strain appears to show up-regulation of more genes rather than induction of a distinct set of genes within the categories shown in Fig. 1E. (For a complete list of genes, see Tables S1 to S3 in the supplemental material.) There is a striking difference between these two strains, however, in the number of induced genes coding for products in energy production and conversion. The *dam* strain displays a high number of induced genes falling under this category, whereas the *dam mutS* strain does not (Fig. 1E). Therefore, it appears that MutS deficiency in a *dam* mutant background reduces the number of induced genes in this category as well as decreases the overall number of transcriptional changes. This effect of MutS is only observed in the *dam* background, as *mutS E. coli* closely resembles the wild type and shows transcriptional changes for only 17 genes. The transcriptional changes observed in the mutant strains are not attributable to different growth stages, as all four strains showed similar growth rates in culture at the time RNA was isolated (data not shown).

***dam* and *dam mutS* strains display constitutive SOS and up-regulation of genes involved in DNA recombination and repair.** The SOS response is induced when RecA is activated in the presence of single-stranded DNA (60). Activated RecA then facilitates the autocleavage of the LexA repressor and the transcriptional activation of those genes whose operons are normally bound and repressed by LexA. Our microarray data show that several LexA-regulated genes are induced in *dam* and to a lesser extent in *dam mutS E. coli*. The analysis shows that the genes *lexA*, *recA*, and *yebG* are all induced at least twofold in the *dam* strain compared to the wild type ($P \leq 0.001$, Table 2). The LexA-regulated genes *sulA* and *recN* also show induction in the *dam* strain, with signal log ratios (*dam*/wild type) of 0.95 ($P = 0.004$) and 0.762 ($P = 0.022$), respectively. Many of these genes (*lexA*, *recN*, *sulA*, and *yebG*) are also induced in the *dam mutS* strain (Table 2). The SOS genes involved in nucleotide excision repair (*uvrA*, *uvrB*, and the recently characterized gene *cho* [39]) do not show induction in the *dam* and *dam mutS* strains by microarray analysis, although our RT-PCR results show that the *cho* gene is expressed at a significantly higher level in the *dam* strain than in the wild type (see below and Table 2).

RecN, a protein known to be involved in DSB repair (22, 50), is not required for *dam* mutant survival as *dam recN* mutants are viable (48). However, we find that *recN* is significantly induced in the *dam* and *dam mutS* strains. We also see a moderate but significant ($P < 0.05$) induction of a non-SOS gene, *recG*, in the *dam* strain (signal log ratio = 0.300, $P = 0.013$). The RecG helicase catalyzes branch migration of three- and four-stranded DNA junctions in vitro and is proposed to catalyze fork regression in vivo (34, 35, 51); RecG has been shown to be important for tolerating DSBs (22, 37) and may be required for *dam* mutant viability (27).

Several other genes involved in recombinational repair show unique up-regulation in *dam* and *dam mutS E. coli*. The primosomal gene *priB* shows up-regulation in these strains. PriB is a structural protein of the primosome, which allows replication restart at recombination intermediates including sites of template damage where the replication fork collapses (40, 54). The genes coding for the subunits of the *E. coli* histone-like protein (HU), *hupA* and *hupB*, are also induced in Dam-deficient *E. coli*. HU is involved in recombinational repair (14, 23), and *hupAB* double mutants are hypersensitive to both gamma irradiation (6) and UV-induced damage (23).

We performed semiquantitative real-time PCR to confirm the gene expression changes we observed by microarray analysis. For the RT-PCR studies, we isolated total RNA from three independent replicates using the same procedure we used for the microarray experiments. After DNase digestion, cDNA for each sample of isolated total RNA was made using random hexamer primers and reverse transcriptase, and controls with no reverse transcriptase were performed for each sample to ensure that genomic DNA was removed by digestion. To determine the relative expression levels for a particular gene, all cDNA samples and no-reverse-transcriptase controls were run in the same assay along with samples for a standard curve. We accounted for variation between samples by normalizing the expression level of each gene in a sample to the amount of housekeeping gene message (*gapA*) in that sample. After normalization to the *gapA* level, we set the expression level for each gene detected in the wild type to a value of 1 and adjusted the expression levels in the other strains accordingly (Fig. 2). We performed Student's *t* test to compare the amount of transcript measured in a mutant strain to the amount in the wild type, and comparisons for which *P* is ≤0.05

TABLE 2. Differential basal gene expression (mutant/wild type) of several SOS response genes and other genes involved in DNA maintenance determined by microarray analysis and RT-PCR[a]

Gene name (Blattner no.)	Signal log ratio					
	Array (ANOVA *P* value)			RT-PCR (*t* test *P* value)		
	dam/WT	*dam mutS*/WT	*mutS*/WT	*dam*/WT	*dam mutS*/WT	*mutS*/WT
lexA-regulated SOS response						
lexA (b4043)	1.56 (0.001)	0.914 (0.051)	0.223 (0.498)	0.970 (0.009)	0.997 (0.023)	0.283 (0.238)
recA (b2699)	2.02 (0.000)	1.69 (0.000)	0.348 (0.278)	1.19 (0.001)	0.986 (0.088)	−0.009 (0.491)
recN (b2616)	0.752 (0.022)	0.835 (0.008)	0.269 (0.350)	1.66 (0.013)	1.53 (0.015)	−0.593 (0.278)
sulA (b0958)	0.950 (0.004)	0.784 (0.010)	0.232 (0.427)	1.47 (0.004)	0.870 (0.068)	−0.086 (0.424)
yebG (b1848)	1.60 (0.001)	1.14 (0.001)	0.049 (0.856)	1.72 (0.046)	1.59 (0.012)	0.314 (0.305)
ruvA (b1861)	0.240 (0.541)	0.182 (0.784)	0.227 (0.553)	1.21 (0.002)	1.09 (0.073)	0.317 (0.147)
ruvB (b1860)	0.094 (0.843)	−0.159 (0.569)	0.107 (0.802)	1.12 (0.003)	1.07 (0.005)	0.584 (0.113)
dinI (b1061)	0.652 (0.091)	0.448 (0.232)	0.360 (0.446)	1.32 (0.002)	0.420 (0.256)	−0.832 (0.135)
uvrA (b4058)	−0.277 (0.240)	−0.308 (0.195)	−0.121 (0.584)	0.637 (0.041)	0.669 (0.060)	0.441 (0.166)
uvrB (b0779)	−0.155 (0.468)	−0.095 (0.671)	0.273 (0.283)	0.966 (0.047)	0.821 (0.064)	0.327 (0.231)
chol ydjQ (b1741)	−0.150 (0.520)	−0.156 (0.331)	−0.133 (0.414)	1.52 (0.014)	0.974 (0.050)	0.275 (0.210)
DNA repair or replication restart (non-SOS)						
priA (b3935)	0.026 (0.872)	−0.317 (0.162)	−0.197 (0.332)	0.071 (0.300)	−0.283 (0.290)	−0.264 (0.319)
priB (b4201)	2.19 (0.001)	1.63 (0.018)	0.356 (0.502)	0.874 (0.055)	0.813 (0.073)	0.509 (0.218)
hupA (b4000)	1.04 (0.015)	0.209 (0.555)	0.100 (0.859)	−0.219 (0.355)	0.269 (0.324)	−0.034 (0.474)
hupB (b0440)	1.89 (0.001)	1.60 (0.003)	0.523 (0.176)	0.556 (0.023)	0.283 (0.296)	0.114 (0.314)

[a] Signal log ratios represent the log of expression ratios (mutant/wild type [WT]), base 2. Therefore, a signal log ratio of 1 is equivalent to a two-fold change in expression level. The genes listed were tested by both array and RT-PCR. ANOVA values were determined using the array analyzer module in S-Plus and represent the significance for expression differences between mutant strains and the wild type. Student's *t* test was performed to compare the expression values of a given gene measured by RT-PCR in mutant versus wild-type strains.

are designated in Fig. 2 by an asterisk. Our RT-PCR results confirm the microarray data and show that the SOS response genes *recA*, *lexA*, *sulA*, *dinI*, and *yebG* are all expressed at higher levels in the *dam* mutant compared to the wild type, while the genes *lexA* and *yebG* are also expressed at a significantly higher level in the *dam mutS* mutant than in wild-type *E. coli* (Fig. 2A). We also used real-time RT-PCR to measure the levels of other SOS genes involved in recombinational repair and show that the genes *recN*, *ruvA*, and *ruvB* are highly expressed in *dam* and *dam mutS* strains compared to the wild type (Fig. 2B). The *uvrC* homologue, *cho*, which has been shown to be up-regulated as part of the SOS response (15), is also significantly induced in the *dam* strain (Fig. 2C). The SOS response genes are not induced in *mutS E. coli*.

The relative expression changes determined by array and RT-PCR correlate as to the direction of change for the LexA-regulated genes discussed. Expression changes measured by these methods, however, do not always show the same absolute magnitudes of change. In most cases RT-PCR detected slightly lower magnitudes of change. For example, in *dam E. coli*, the SOS gene displaying the highest level of induction by microarray analysis is *recA* (fourfold induction), while RT-PCR detected a twofold induction of *recA* in *dam* compared to the wild type (Table 2). In general, however, our levels of SOS response gene induction in *dam* cells compared to the wild type are consistent with those determined by Peterson et al. (49) using the β-galactosidase reporter assay. The RT-PCR data also confirm the microarray data in showing that the non-SOS genes *priB* and *hupB* are moderately induced in *dam E. coli*.

Dam-deficient *E. coli* strains exhibit a higher level of DSBs. We performed neutral single-cell microgel electrophoresis to determine the levels of DSBs in the genomes of wild-type, *dam*, *dam mutS*, and *mutS* mutant cells. Using the single-cell electrophoresis method developed by Singh et al. (57, 58), we were able to detect a single double-strand break in the genome of a cell. We assume that one linear tail corresponds to a single double-strand break (4), as shown in Fig. 3A; an individual cell with no DSBs appears as a head with no tail, whereas a cell with DSBs appears as a head followed by linear tails indicative of the number of breaks in the genome. For these experiments, cultures were grown as described above for the gene expression studies, and three independent experiments were performed. A total of 600 to 1,000 single cells for each strain were analyzed by Komet analysis software (Kinetic Imaging Ltd.) and by the visual counting of the number of DSBs. Our data show that Dam-deficient *E. coli* strains have a significantly higher level of basal DSBs (Mann-Whitney U test, $P < 0.02$) than the level of DSBs in the wild-type strain, with *dam* cells having on average 1.2 breaks per cell (Fig. 3B). The *dam mutS* and *mutS* strains do not show a significantly higher level of double-strand breaks compared to the wild type.

Although the average number of DSBs detected in the *dam* strain is 1.2 breaks per cell, we observe a broad range of breaks per cell. A small percentage of the *dam* cells (6%) show between 5 and 12 double-strand breaks, while 42% of the cells show no DSBs and the majority of cells display between 1 and 4 DSBs. We expect that this broad range in the number of DSBs is due to differences in the cell population with respect to the number of active DNA replication forks and the stages of recombination substrates in each cell. In other words, DSBs are lethal lesions and most likely do not persist for long in the cells, and therefore we were able to capture relatively few cells with a high level of damage that had not yet completed recombinational repair. The short persistence of DSBs in the cells

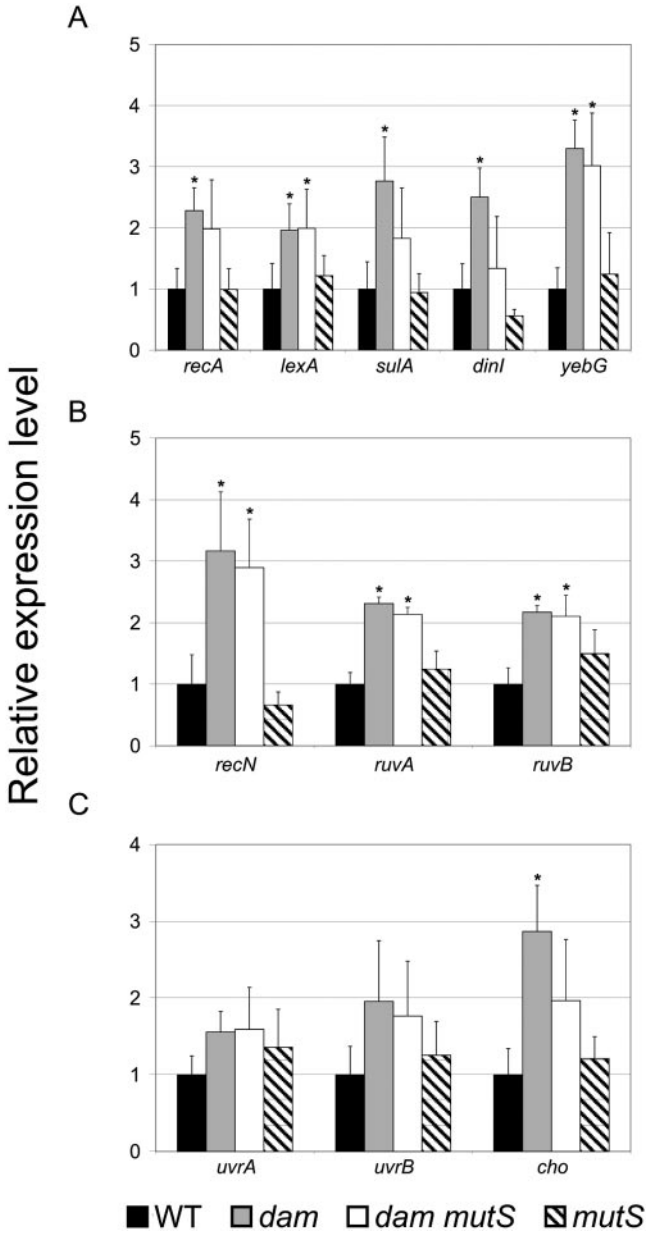

FIG. 2. Relative expression levels for several SOS genes determined by semiquantitative real-time PCR. Student's *t* tests were performed to compare the transcript levels of a gene detected in a mutant strain to the level detected in the wild type. Comparisons for which *P* is ≤0.05 are designated by an asterisk, and error bars represent standard deviation. The SOS response genes represented include genes involved in SOS regulation (A), recombination (B), and nucleotide excision repair (C).

would explain why previous studies could only detect DSBs in *dam rec* double-mutant strains deficient in recombinational repair and were unable to detect DSBs in *dam*-only mutant cells (41, 47). The other strains did not show a broad range of DSB formation: 80 to 90% of the cells showed no DSBs, while one to three DSBs were detected in the remaining cells.

Komet image analysis software analyzes photometric data and quantifies the fluorescence of the head and tail. The software provides measurements such as the mean intensities of the head and tail and the tail length. Percent DNA in the head or tail represents a percentage of the total measured intensity (head and tail), and cells with a higher level of DNA damage will display a higher percentage of tail DNA. Figure 3C shows a box plot of the distribution of cells for each strain according to the percentage of tail DNA. The horizontal line in each box represents the median of the data, while the box represents the interquartile range, or the range including 50% of the data. The lines extending from the top and bottom of each box mark the minimum and maximum values within the data set that fall within an acceptable range, and any values outside of this range (outliers) are displayed as individual points. The *dam* cells display the broadest range of data, with many cells showing a very high percentage of DNA in the tail. The distributions of cells by percent tail DNA are similar for the wild-type, *dam mutS*, and *mutS* strains, although *dam mutS* cells show a few outliers with a high level of damage. The data support the idea that mismatch repair induces DSBs in *dam* cells and causes a high level of damage; while only a subset of *dam* mutant cells exhibit very high levels of damage, we speculate that the lethal damage is repaired efficiently and does not persist for long in the cells, resulting in a majority of the cells showing lower levels of damage.

DISCUSSION

Dam-deficient *E. coli* strains exhibit pleiotropic changes, including an increased mutation rate, uncoordinated DNA replication initiation, and transcriptional alterations (24, 32, 45). Many of these phenotypes result from the absence of hemimethylated DNA following passage of the replication fork. Dam-deficient *E. coli* strains also exhibit a hypersensitivity to DNA damage and a dependence on recombinational repair, and both phenotypes can be suppressed by inactivating mismatch repair (16, 36, 62). In the present study, we determined the global transcriptional changes in *dam*, *dam mutS*, and *mutS E. coli* strains. Our data show that *dam* and *dam mutS* strains exhibit the greatest number of transcriptional changes compared to the wild type. Although gene expression can be regulated by Dam methylation, most of the gene expression changes observed in these strains appear to be due to secondary effects of Dam deficiency rather than from direct methylation-mediated gene regulation. The majority of genes induced in *dam* and *dam mutS* strains are genes encoding products of carbohydrate transport and metabolism, translation, and, in the *dam* strain, energy production and conversion. The up-regulation of genes involved in metabolism, energy production, and translation in *dam E. coli* may be indicative of the great effort this strain must devote to growth and to coping with asynchronous DNA replication and DNA damage. We also see induction of several *lexA*-regulated genes in *dam* and *dam mutS* strains, which is consistent with the previous findings of others (43, 44, 49). Furthermore, mismatch repair appears to be contributing to the transcriptional changes observed in the *dam* strain; adding a mutation in *mutS* suppresses many of the gene expression changes in the *dam* strain, as the *dam mutS* strain shows induction of fewer genes in categories such as amino acid and carbohydrate transport and metabolism, energy production and conversion, and translation. Our data suggest that due to the many functions of adenine methylation,

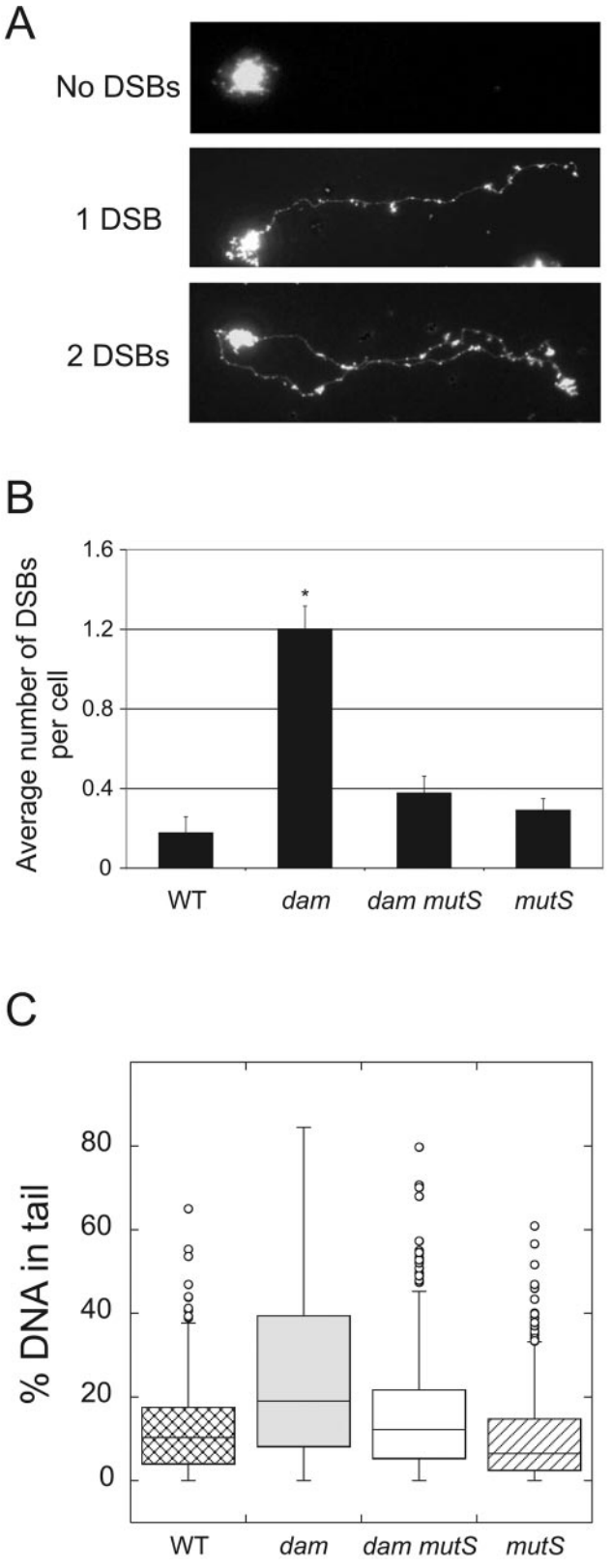

FIG. 3. *E. coli* strains analyzed by single-cell microgel electrophoresis. Six hundred to 1,000 individual cells for each strain were analyzed by visually counting the number of breaks and by Komet analysis software (Kinetic Imaging Ltd.) (A) Representative pictures of individual cells analyzed by microgel electrophoresis. Cells with no tails indicate no DSBs in the genome, whereas cells with tails indicate the number of strand breaks in the genome. (B) Number of DSBs per cell for each strain determined by counting the tails of each cell for each of the strains. WT, wild type. Error bars represent standard error. *, Mann-Whitney U test ($P < 0.02$). (C) Results from Komet analysis. The percentage of DNA in the tail represents a percentage of the total DNA (total fluorescence) detected in both the head and tail. A box plot shows the distribution of cell data for each strain. Horizontal lines for each box represent the median value, with the box representing 50% of the data (box upper and lower limits represent the upper and lower quartiles, respectively). Vertical lines extending from the box show the full range of data, and outliers are shown as individual points (outliers are defined as values greater than the upper quartile + 1.5 × interquartile distance).

a deficiency in Dam increases the overall stress level in the cells, including stress caused by DNA damage, and that introducing an additional mutation in mismatch repair abrogates some of this stress. A deficiency in MutS alone does not result in many changes at the transcriptional level.

Two previous studies have examined the effects of Dam methylation on global gene expression patterns. Løbner-Olesen et al. (25) found few gene expression changes in Dam-deficient strains that were either *dam* null or that expressed 30% of the level of Dam relative to the wild type. However, their study showed that Dam overexpression resulted in altered expression of numerous genes, and the effects of Dam overproduction were almost identical to the gene expression effects they observed in *seqA* mutant cells or cells in which reinitiation of replication occurs at *oriC* repeatedly during a single replication cycle (9, 59). Because most of the genes whose expression was altered did not contain d(GATC) sites in their promoter regions, the authors proposed that the gene expression changes observed in Dam-overproducing and *seqA* mutant strains are due to the increased amount of fully methylated DNA and the resulting alterations in chromosome structure. Although their study did not find many gene expression changes in the *dam*-null strain compared to the wild type, their findings are similar to ours in the respect that Dam methylation appears to have little direct effect on gene regulation. The second study by Oshima et al. (44) tested the gene expression changes in *dam* mutant cells under aerobic and low aerobic conditions. Their study, like ours, found many gene expression changes in the Dam-deficient strain. Furthermore, genes involved in amino acid metabolism, energy metabolism, and the environmental stress response were up-regulated in the *dam* mutant under aerobic conditions, which is consistent with our data.

Our data show that several SOS response genes are constitutively induced in the *dam* and *dam mutS* strains. Dam-deficient strains have a high basal level of single-strand breaks compared to the wild type (30), and thus single-strand breaks may be the primary SOS-inducing signal. Previous work has indicated that damage in *dam* strains also consists of DSBs; expression of *recA*, *recB*, *recC*, *ruvA*, *ruvB*, and *ruvC* is essential for *dam* mutant viability, although expression of *recN*, *recO*, *recF*, and *recR* is not required (27, 49). Furthermore, the presence of DSBs and the requirement for DSB recombinational repair are dependent on functional mismatch repair; Wang and Smith (62) have shown that mutations in mismatch repair

(*mutS* or *mutL*) suppress the formation of DSBs and the requirement for recombination in a *dam rec* background. However, the basal level of DSBs in *dam* mutants has not been measured in recombination-proficient strains. Using a single-cell assay where we can detect a single DSB per cell, we measured the level of DSBs in *dam* and *dam mutS E. coli* strains that are proficient in recombinational repair. Based on our data, *dam E. coli* strains have on average 1.2 double-strand breaks per cell, whereas wild-type and *dam mutS* strains have an average of 0.17 and 0.37 DSB per cell, respectively. Therefore, while inactivating MutS abrogates the need for DSB repair in *dam* mutant cells, we propose that mismatch repair contributes to nearly all of the DSBs detected in *dam* cells.

It is important to note that one phenotype of *dam* mutants is asynchronous cell division and multiple firings of the origin of replication during the cell cycle (24, 52). Such multiple firings may lead to hyperploidy and an increase in DNA fragments as multiple DNA duplexes are being synthesized. Thus, the number of tails in Dam-deficient strains may be higher due to this phenotype. The contributions of multiple DNA molecules within the cell, however, should be the same for both *dam* and *dam mutS* mutant strains as both strains lack DNA adenine methylation. While the level of DSBs is higher in *dam* mutants than it is in *dam mutS* mutant cells, DSB formation in *dam* mutants is therefore dependent on mismatch repair.

As mentioned in the Results section, we believe the level of mismatch-repair-induced DSBs in the *dam* strain to be well above the average of 1.2 breaks per cell. Because we observed a broad range of values, with the highest level reaching 12 breaks in a *dam* cell, we speculate that the DSBs are repaired efficiently and do not persist for long in the cells, and thus we could only capture a small population of cells with unrepaired DSBs. This scenario would explain why other methods, such as neutral sucrose gradients (62) and pulsed-field gel electrophoresis (41), could only detect an increased level of DSBs in *dam rec* backgrounds. Our results are also consistent with the findings of McCool et al. (33) demonstrating that SOS expression in *dam* mutant cells follows a two-population model in which some cells show high SOS expression while other cells do not; our data show that at least one form of DNA damage—DSB formation—in *dam* mutant cells is stochastically formed and is not present at uniform levels in the culture at a given moment in time.

Despite the aforementioned correlative data on DSB formation, the dependence on recombination, and functional mismatch repair in a *dam* mutant strain, SOS induction is not suppressed by an additional mutation in *mutS*. Therefore, other SOS-inducing signals must be present in *dam* and *dam mutS* strains. While recombinational repair, and specifically DSB repair, is required for *dam* mutant viability (27, 48), induction of SOS is also critical for survival, and *lexA dam* double mutants in which the LexA repressor cannot be inactivated are inviable (49).

The mechanism by which mismatch repair induces DSBs in the absence of Dam methylation is not fully understood. Mismatch repair may be making dual incisions at unmethylated d(GATC) sites, forming DSBs (1, 17). Alternatively, MutH-catalyzed single incisions could result in DSBs when these single-strand nicks are encountered by a replication fork, resulting in replication fork collapse and a DSB (see reference 27 for a discussion of this model). To account for the increased level of DSBs observed in *dam* mutant cells, MutH would need to make more single-strand incisions in *dam* mutant cells than in *dam*$^+$ cells. Increased MutH-catalyzed single-strand incisions may occur in *dam* mutant cells because of the higher presence of MutH substrate or unmethylated d(GATC) sites, and an increased level of single-strand breaks has indeed been observed in *dam* cells (30). In growing *dam* mutant cells, therefore, the coupling of a high presence of single-strand gaps with multiple replication forks may result in replication fork collapse and may account for the increased level of DSBs observed in the *dam* strain. Under this model and based on our results, the frequency at which replication forks encounter single-strand gaps in *dam E. coli* could result in as many as 10 or more DSBs. However, due to the up-regulation of recombinational repair in this strain, *dam* mutant cells efficiently repair these DSBs, and thus the average level of DSBs observed in the culture is only one to two breaks per cell. Unlike the first model where MutH catalyzes two incisions on complementary strands resulting in a DSB, the second model relies on replication for the formation of DSBs. The replication dependence of DSB formation and recombination in *dam* mutant cells is currently being tested.

The present study demonstrates the importance of functional mismatch repair in contributing to DNA damage and gene expression changes in *dam* mutant cells. We have shown that DSB formation in *dam* mutant cells is dependent on functional mismatch repair; *dam* mutant cells have a higher level of DSBs than the wild type, whereas *dam mutS* and *mutS* mutant cells do not. We have also shown that the SOS response and genes involved in recombinational repair are induced in *dam* mutant *E. coli*. While it has been shown that mismatch repair sensitizes cells to DNA-damaging agents in a *dam* mutant background (16), the high level of mismatch-repair-induced basal damage in *dam* mutant cells helps explain why this strain is hypersensitive to DNA-damaging agents. We are currently examining the role of mismatch repair in mediating toxicity to exogenous DNA-damaging agents, using the strains characterized in this study.

ACKNOWLEDGMENTS

We would like to acknowledge Sanchita Battacharya and Rebecca Fry from the Biomicro Center, MIT, for their help with microarray data analysis. In addition, we would like to thank Narendra Singh for his helpful suggestions in performing the neutral single-cell microgel electrophoresis as well as Susan Wallace in interpreting the microgel data. We would also like to thank Leona Samson for providing the fluidics station and scanner necessary for performing Affymetrix microarray analysis. Finally, we would like to thank Charles Morton for his help with statistical analysis and Yuriy Alekseyev for his careful reading of the manuscript.

This work was funded by National Institute of Health (NIH) grants 5-R01-CA86061, 1-R01-CA-80024, and GM63790, NIH/National Institute of General Medical Sciences grant 2-T32-GM08334, and National Institute of Environmental Health Sciences grant 1-P01-ES-11399.

REFERENCES

1. **Au, K. G., K. Welsh, and P. Modrich.** 1992. Initiation of methyl-directed mismatch repair. J. Biol. Chem. **267:**12142–12148.
2. **Bakker, A., and D. W. Smith.** 1989. Methylation of GATC sites is required for precise timing between rounds of DNA replication in *Escherichia coli*. J. Bacteriol. **171:**5738–5742.
3. **Bell, D. C., and C. G. Cupples.** 2001. Very-short-patch repair in *Escherichia coli* requires the *dam* adenine methylase. J. Bacteriol. **183:**3631–3635.

4. **Blaisdell, J. O., and S. S. Wallace.** 2001. Abortive base-excision repair of radiation-induced clustered DNA lesions in *Escherichia coli*. Proc. Natl. Acad. Sci. USA **98:**7426–7430.
5. **Bolstad, B. M., R. A. Irizarry, M. Astrand, and T. P. Speed.** 2003. A comparison of normalization methods for high density oligonucleotide array data based on variance and bias. Bioinformatics **19:**185–193.
6. **Boubrik, F., and J. Rouviere-Yaniv.** 1995. Increased sensitivity to γ irradiation in bacteria lacking protein HU. Proc. Natl. Acad. Sci. USA **92:**3958–3962.
7. **Braaton, B. A., X. Nuo, L. S. Kaltenbach, and D. A. Low.** 1994. Methylation patterns in *pap* regulatory DNA control pyelonephritis-associated pili phase variation in *E. coli*. Cell **76:**577–588.
8. **Braun, R. E., and A. Wright.** 1986. DNA methylation differentially enhances the expression of one of the two *E. coli* dnaA promoters in vivo and in vitro. Mol. Gen. Genet. **202:**246–250.
9. **Brendler, T., J. Sawitzke, K. Sergueev, and S. Austin.** 2000. A case for sliding SeqA tracts at anchored replication forks during *Escherichia coli* chromosome replication and segregation. EMBO J. **19:**6249–6258.
10. **Cooper, D. L., R. S. Lahue, and P. Modrich.** 1993. Methyl-directed mismatch repair is bidirectional. J. Biol. Chem. **268:**11823–11829.
11. **Correnti, J., V. Munster, T. Chan, and M. van der Woude.** 2002. Dam-dependent phase variation of Ag43 in *Escherichia coli* is altered in a *seqA* mutant. Mol. Microbiol. **44:**521–532.
12. **d'Alençon, E., A. Taghbalout, C. Bristow, R. Kern, R. Aflalo, and M. Kohiyama.** 2003. Isolation of a new hemimethylated DNA binding protein which regulates *dnaA* gene expression. J. Bacteriol. **185:**2967–2971.
13. **DeWitt, S. K., and E. A. Adelberg.** 1962. The occurrence of a genetic transposition in a strain of *Escherichia coli*. Genetics **47:**577–586.
14. **Dri, A.-M., P. L. Moreau, and J. Rouviere-Yaniv.** 1992. Role of the histone-like proteins OsmZ and Hu in homologous recombination. Gene **120:**11–16.
15. **Fernandez de Henestrosa, A. R., T. Ogi, S. Aoyagi, D. Chafin, J. J. Hayas, H. Ohmori, and R. Woodgate.** 2000. Identification of additional genes belonging to the LexA regulon in *Escherichia coli*. Mol. Microbiol. **35:**1560–1572.
16. **Fram, R. J., P. S. Cusick, J. M. Wilson, and M. G. Marinus.** 1985. Mismatch repair of cis-diamminedichloroplatinum(II)-induced DNA damage. Mol. Pharmacol. **28:**51–55.
17. **Glickman, B. W., and M. Radman.** 1980. *Escherichia coli* mutator mutants deficient in methylation-instructed DNA mismatch correction. Proc. Natl. Acad. Sci. USA **77:**1063–1067.
18. **Grilley, M., J. Griffith, and P. Modrich.** 1993. Biodirectional excision in methyl-directed mismatch repair. J. Biol. Chem. **268:**11830–11837.
19. **Henaut, A., T. Rouxel, A. Gleizes, I. Moszer, and A. Danchin.** 1996. Uneven distribution of GATC sequence motifs in the *Escherichia coli* chromosome, its plasmids and its phages. J. Mol. Biol. **257:**574–585.
20. **Herman, G. E., and P. Modrich.** 1981. *Escherichia coli* K-12 clones that overproduce *dam* methylase are hypermutable. J. Bacteriol. **145:**644–646.
21. **Irizarry, R. A., B. M. Bolstad, F. Collin, L. M. Cope, B. Hobbs, and T. P. Speed.** 15 February 2003, posting date. Summaries of Affymetrix GeneChip probe level data. Nucleic Acids Res. **31:**e15. [Online.] doi:10.1093/nar/gng015.
22. **Kosa, J. L., Z. Z. Zdraveski, S. Currier, M. G. Marinus, and J. M. Essigmann.** 2004. RecN and RecG are required for *Escherichia coli* survival of bleomycin-induced damage. Mutat. Res. **554:**149–157.
23. **Li, S., and R. Waters.** 1998. *Escherichia coli* strains lacking protein HU are UV sensitive due to a role for HU in homologous recombination. J. Bacteriol. **180:**3750–3756.
24. **Løbner-Olesen, A., F. G. Hansen, K. V. Rasmussen, B. Martin, and P. L. Kuempel.** 1994. The initiation cascade for chromosome replication in wild-type and Dam methyltransferase deficient *Escherichia coli* cells. EMBO J. **13:**1856–1862.
25. **Løbner-Olesen, A., M. G. Marinus, and F. G. Hansen.** 2003. Role of SeqA and Dam in *Escherichia coli* gene expression: a global/microarray analysis. Proc. Natl. Acad. Sci. USA **100:**4672–4677.
26. **Marinus, M. G.** 1985. DNA methylation influences trpR promoter activity in *Escherichia coli* K-12. Mol. Gen. Genet. **200:**185–186.
27. **Marinus, M. G.** 2000. Recombination is essential for viability of an *Escherichia coli dam* (DNA adenine methyltransferase) mutant. J. Bacteriol. **182:**463–468.
28. **Marinus, M. G.** 1976. Adenine methylation of Okazaki fragments in *Escherichia coli*. J. Bacteriol. **128:**853–854.
29. **Marinus, M. G., and E. B. Konrad.** 1976. Hyper-recombination in *dam* mutants of *Escherichia coli* K-12. Mol. Gen. Genet. **149:**273–277.
30. **Marinus, M. G., and N. R. Morris.** 1974. Biological function for 6-methyladenine residues in the DNA of *Escherichia coli* K12. J. Mol. Biol. **85:**309–322.
31. **Marinus, M. G., and N. R. Morris.** 1975. Pleiotropic effects of a DNA adenine methylation mutation (dam-3) in *Escherichia coli* K12. Mutat. Res. **28:**15–26.
32. **Marinus, M. G., A. Poteete, and J. A. Arraj.** 1984. Correlation of DNA adenine methylase activity with spontaneous mutability in *Escherichia coli* K-12. Gene **28:**123–125.
33. **McCool, J. D., E. Long, J. F. Petrosino, H. A. Sandler, S. M. Rosenberg, and S. J. Sandler.** 2004. Measurement of SOS expression in individual *Escherichia coli* K-12 cells using fluorescence microscopy. Mol. Microbiol. **53:**1343–1357.
34. **McGlynn, P., and R. G. Lloyd.** 1999. RecG helicase acitivity at three- and four-strand DNA structures. Nucleic Acids Res. **27:**3049–3056.
35. **McGlynn, P., and R. G. Lloyd.** 2001. Rescue of stalled replication forks by RecG: simultaneous translocation on the leading and lagging strand templates supports an active DNA unwinding model for fork reversal and Holliday junction formation. Proc. Natl. Acad. Sci. USA **98:**8227–8234.
36. **McGraw, B. R., and M. G. Marinus.** 1980. Isolation and characterization of Dam+ revertants and suppressor mutations that modify secondary phenotypes of dam-3 strains of *Escherichia coli* K-12. Mol. Gen. Genet. **178:**309–315.
37. **Meddows, T. R., A. P. Savory, and R. G. Lloyd.** 2004. RecG helicase promotes DNA double-strand break repair. Mol. Microbiol. **52:**119–132.
38. **Modrich, P.** 1989. Methyl-directed DNA mismatch correction. J. Biol. Chem. **264:**6597–6600.
39. **Moolenaar, G. F., S. van Rossum-Fikkert, M. van Kesteren, and N. Goosen.** 2002. Cho, a second endonuclease involved in *Escherichia coli* nucleotide excision repair. Proc. Natl. Acad. Sci. USA **99:**1467–1472.
40. **Ng, J. Y., and K. J. Marians.** 1996. The ordered assembly of the ϕX174-type primosome. I. Isolation and identification of intermediate protein-DNA complexes. J. Biol. Chem. **271:**15642–15648.
41. **Nowosielska, A., and M. G. Marinus.** 2005. Cisplatin induces DNA double-strand break formation in *Escherichia coli dam* mutants. DNA Repair (Amsterdam) **4:**773–781.
42. **Ogden, G. B., M. J. Pratt, and M. Schaechter.** 1988. The replicative origin of the *E. coli* chromosome binds to cell membranes only when hemimethylated. Cell **54:**127–135.
43. **O'Reilly, E. K., and K. N. Kreuzer.** 2004. Isolation of SOS constitutive mutants of *Escherichia coli*. J. Bacteriol. **186:**7149–7160.
44. **Oshima, T., C. Wada, Y. Kawagoe, T. Ara, M. Maeda, Y. Masuda, S. Hiraga, and H. Mori.** 2002. Genome-wide analysis of deoxyadenosine methyltransferase-mediated control of gene expression in *Escherichia coli*. Mol. Microbiol. **45:**673–695.
45. **Palmer, B. R., and M. G. Marinus.** 1994. The *dam* and *dcm* strains of *Escherichia coli*—a review. Gene **143:**1–12.
46. **Parker, B., and M. G. Marinus.** 1988. A simple and rapid method to obtain substitution mutations in *Escherichia coli*: isolation of a dam deletion/insertion mutation. Gene **73:**531–535.
47. **Parker, B. O., and M. G. Marinus.** 1992. Repair of DNA heteroduplexes containing small heterologous sequences in *Escherichia coli*. Proc. Natl. Acad. Sci. USA **89:**1730–1734.
48. **Peterson, K. R., and D. W. Mount.** 1993. Analysis of the genetic requirements for viability of *Escherichia coli* K-12 DNA adenine methylase (*dam*) mutants. J. Bacteriol. **175:**7505–7508.
49. **Peterson, K. R., K. F. Wertman, D. W. Mount, and M. G. Marinus.** 1985. Viability of *Escherichia coli* K-12 DNA adenine methylase (dam) mutants requires increased expression of specific genes in the SOS regulon. Mol. Gen. Genet. **201:**14–19.
50. **Picksley, S. M., P. V. Attfield, and R. G. Lloyd.** 1984. Repair of double-strand breaks in *Escherichia coli* K12 requires a functional *recN* product. Mol. Gen. Genet. **195:**267–274.
51. **Robu, M. E., R. B. Inman, and M. M. Cox.** 2004. Situational repair of replication forks: roles of RecG and RecA proteins. J. Biol. Chem. **279:**10973–10981.
52. **Russell, D. W., and N. Zinder.** 1987. Hemimethylation prevents DNA replication in *E. coli*. Cell **50:**1071–1079.
53. **SaiSree, L., M. Reddy, and J. Gowrishankar.** 2000. *lon* incompatability associated with mutations causing SOS induction: null *uvrD* alleles induce an SOS response in *Escherichia coli*. J. Bacteriol. **182:**3151–3157.
54. **Sandler, S. J.** 2000. Multiple genetic pathways for restarting DNA replication forks in *Escherichia coli* K-12. Genetics **155:**487–497.
55. **Schlagman, S. L., S. Hattman, and M. G. Marinus.** 1986. Direct role of the *Escherichia coli* Dam DNA methyltransferase in methylation-directed mismatch repair. J. Bacteriol. **165:**896–900.
56. **Singh, N. P.** 2000. Microgels for estimation of DNA strand breaks, DNA protein crosslinks and apoptosis. Mutat. Res. **455:**111–127.
57. **Singh, N. P., M. T. McCoy, R. R. Tice, and E. L. Schneider.** 1988. A simple technique for quantitation of low levels of DNA damage in individual cells. Exp. Cell Res. **175:**184–191.
58. **Singh, N. P., R. E. Stephens, H. Singh, and H. Lai.** 1999. Visual quantification of DNA double-strand breaks in bacteria. Mutat. Res. **429:**159–168.
59. **Slater, S., S. Wold, M. Lu, E. Boye, K. Skarstad, and N. Kleckner.** 1995. *E. coli* SeqA protein binds oriC in two different methyl-modulated reactions appropriate to its roles in DNA replication initiation and origin sequestration. Cell **82:**927–936.
60. **Walker, G. C.** 1987. The SOS response of *Escherichia coli*, p. 1346–1357. *In* F. C. Neidhardt, J. L. Ingraham, K. B. Low, B. Magasanik, M. Schaechter,

and H. E. Umbarger (ed.), *Escherichia coli* and *Salmonella typhimurium*: cellular and molecular biology, vol. 2. American Society for Microbiology, Washington, D.C.

61. **Wallecha, A., V. Munster, J. Correnti, T. Chan, and M. van der Woude.** 2002. Dam- and OxyR-dependent phase variation of *agn43*: essential elements and evidence for a new role of DNA methylation. J. Bacteriol. **184:**3338–3347.
62. **Wang, T.-C. V., and K. C. Smith.** 1986. Inviability of *dam recA* and *dam recB* cells of *Escherichia coli* is correlated with their inability to repair DNA double-strand breaks produced by mismatch repair. J. Bacteriol. **165:**1023–1025.
63. **Welsh, K., A. L. Lu, S. Clark, and P. Modrich.** 1987. Isolation and characterization of the *Escherichia coli mutH* gene product. J. Biol. Chem. **262:** 15624–15629.
64. **Yang, H., E. Wolff, M. Kim, A. Diep, and J. H. Miller.** 2004. Identification of mutator genes and mutational pathways in *Escherichia coli* using a multicopy cloning approach. Mol. Microbiol. **53:**283–295.